

# An impulse radio ultrawideband system for contactless noninvasive respiratory monitoring

Nijsure, Yogesh; Gunawan, Erry; Yang, Zhang; Guan, Yong Liang; Chua, Ai Ping; Wen, Fuxi;  
Tay, Wee Peng

2013

Nijsure, Y., Tay, W. P., Gunawan, E., Wen, F., Yang, Z., Guan, Y. L., & Chua, A. P. (2013). An impulse radio ultrawideband system for contactless noninvasive respiratory monitoring. *IEEE Transactions on Biomedical Engineering*, 60(6), 1509-1517.  
doi:10.1109/TBME.2012.2237401

<https://hdl.handle.net/10356/98236>

<https://doi.org/10.1109/TBME.2012.2237401>

---

© 2013 IEEE. Personal use of this material is permitted. Permission from IEEE must be obtained for all other uses, in any current or future media, including reprinting/republishing this material for advertising or promotional purposes, creating new collective works, for resale or redistribution to servers or lists, or reuse of any copyrighted component of this work in other works. The published version is available at:  
<https://doi.org/10.1109/TBME.2012.2237401>.

*Downloaded on 26 Aug 2022 03:38:52 SGT*

# An Impulse Radio Ultra Wideband System for Contactless Non-invasive Respiratory Monitoring

Yogesh Nijsure<sup>†</sup>, *Student Member, IEEE*, Wee Peng Tay, *Member, IEEE*, Erry Gunawan, *Member, IEEE*, Fuxi Wen, *Member, IEEE*, Zhang Yang, *Student Member, IEEE*, Yong Liang Guan, *Member, IEEE*, and Ai Ping Chua

**Abstract**—We design a impulse radio ultra-wideband (IR UWB) radar monitoring system to track the chest wall movement of a human subject during respiration. Multiple sensors are placed at different locations to ensure that the backscattered signal could be detected by at least one sensor no matter which direction the human subject faces. We design a hidden Markov model (HMM) to infer the subject facing direction and his or her chest movement. We compare the performance of our proposed scheme on 15 human volunteers with the medical gold standard using respiratory inductive plethysmography (RIP) belts, and show that on average, our estimation is over 81% correlated with the measurements of a RIP belt system. Furthermore, in order to automatically differentiate between periods of normal and abnormal breathing patterns, we develop a change point detection algorithm based on perfect simulation techniques to detect changes in the subject’s breathing. The feasibility of our proposed system is verified by both the simulation and experiment results.

**Index Terms**—Ultra-wideband impulse radio radar, respiration monitoring, sleep apnea detection, hidden Markov model.

## I. INTRODUCTION

Obstructive sleep apnea is the most common form of sleep breathing disorder, and occurs when there is partial or complete cessation of airflow due to upper airway obstruction, while ventilatory effort by the patient persists. Sleep apnea affects sleep duration and quality, leading to chronic partial sleep deprivation with consequent well-recognized impaired neuro-cognitive function and daytime performance, increased risk for metabolic and cardiovascular diseases (e.g hypertension, coronary heart disease, life-threatening arrhythmias and stroke) and motor vehicular accidents [1]–[4], and a diminished quality of life. Large prospective cohort community-based studies have also added to the growing evidence that sleep apnea increases risk of death [5], [6].

In order to diagnose sleep apnea and other respiratory and sleep disorders, an overnight polysomnography (PSG) is performed in hospitals. Respiratory inductive plethysmography (RIP) is utilized for measuring the respiratory effort of the patient as shown in [7]. In RIP, elastic belts are worn around the chest or abdomen, and respiratory movements are measured by detecting the change in inductance of the belt due to the respiratory effort. This is an invasive technique for

respiratory monitoring. Overtightening of the belts can impede the patient’s respiratory efforts, and shifting of body position during sleep often leads to loss of signals due to loosening of the belts. The belts also add to physical discomfort and may result in sleep disruption for the patient. The lack of adequate sleep time and loss of data signal may mean that the patient is required to repeat the PSG. Recently there have been new developments such as fabricating capacitive sensors in clothes, which can be worn by the patient in order to facilitate respiratory monitoring [8], [9]. However these methods may produce inaccurate results due to patient movements during sleep or other factors like ambient room conditions. Physical wear and tear of the capacitive sensors embedded in the fabric is also a challenge. Other methods involve the use of unobtrusive sensors and on-body wearable devices in order to measure the respiratory effort [10], [11].

In this paper, we develop a wireless, **contactless** and **non-invasive** respiratory monitoring system that can be used in PSG studies, home respiratory monitoring applications or other applications like physiotherapies. We use ultra-wideband (UWB) signals because its large bandwidth facilitates high time resolution, allowing precise ranging and location estimation. After the US Federal Communication Commission (FCC) approved the limited use of UWB technology, UWB systems have drawn considerable attention for non-contact medical applications [12]. One important application is in sleep monitoring, where measuring the respiratory amplitude and breathing rate is crucial for sleep apnea diagnosis [13], [14]. Various UWB technologies have been studied, including frequency modulated UWB [15], [16], and impulse radio (IR) UWB [17]–[19].

In [18]–[21], the feasibility of using IR UWB for estimating the breathing rate is investigated. The measurement system proposed by [18], [19] consists of two UWB antennas, one for transmission and the other for reception, and are pointed directly at the chest of the human subject. However, the performance of such systems is sensitive to the movement of the subject. Since one fixed antenna is used, if the human subject is not facing the antenna at a sufficiently small angle, the signal backscattering comes mostly from the side of the body instead of from the chest area, resulting in poor estimation accuracy. To solve the problem of the human subject not facing the UWB antenna at a sufficiently small angle, we propose a setup comprising of multiple UWB transceivers. Multiple transmit and receive antennas are placed at different locations to ensure that the backscattered signal can be detected by

This research was supported by a NITHM grant. The first six authors are with the School of Electrical and Electronic Engineering, Nanyang Technological University, Singapore. A.P. Chua is from the Department of Medicine, National University Healthcare System, Singapore. <sup>†</sup> Corresponding author, e-mail: nijsure@ntu.edu.sg

at least one receiver antenna. To fuse the information from the multiple receiver antennas, we develop a hidden Markov model (HMM) based method to estimate the chest movement from the backscattered signals from all receiver antennas. In addition, we present a change point detection algorithm based on perfect simulation techniques to automatically detect the statistical change points at which abnormal breathing patterns are likely to have occurred. Our main contributions are the following.

- 1) We develop a novel HMM for tracking chest wall movements during respiration, based on data fusion from multiple UWB transceivers. This is verified both experimentally and through simulations.
- 2) We compare the performance of the proposed HMM based approach with the medical gold standard using a RIP belt system. We show that our inferred respiratory amplitude is highly correlated with that produced by a RIP belt.
- 3) We develop a change point detection algorithm for detecting abnormal breathing patterns to facilitate automatic sleep disordered breathing detection based on respiratory signals.

The rest of the paper is organized as follows. In Section II, we describe the system architecture and provide a detailed analysis of the proposed HMM approach for tracking the human chest wall motion during respiration. In Section III, we present the change point detection algorithm for detecting abnormal breathing patterns to facilitate sleep apnea detection. In Section IV, we present the simulation and experimental results including the comparison with standard benchmark method for respiration monitoring. Finally, in Section V we provide concluding remarks on the application of the proposed method and its suitability in non-invasive medical applications. Throughout this work, we use  $(\cdot)^T$  to denote matrix transpose. We use  $\mathcal{N}(\mu, \Sigma)$  to denote the (multivariate) Gaussian distribution with mean  $\mu$  and covariance matrix  $\Sigma$ .

## II. SYSTEM MODEL AND CHEST MOVEMENT INFERENCE

### A. System Model

In this section, we describe our experimental UWB monitoring setup. Two pairs of co-located transmit and receive antenna are used in our experiments, as shown in Figure 1. We note that although only two transceiver pairs are used in our setup, our work can be easily extended to cases where more pairs of antennas are utilized. Two UWB impulses generated by a picosecond impulse generator are transmitted simultaneously from the two transmit antennas. For our experimental purposes, the backscattered signals at the receive antennas are detected using a digital oscilloscope and processed by a computer. The human chest wall movement can be estimated by determining the propagation delay and the received signal strength (RSS) of the backscattered UWB signal since the propagation delay is directly proportional to the chest movement, and the signal strength is related to the distance the subject is from the UWB antennas, and the angle she is facing. In the following, we describe the model equations governing the propagation delay and the RSS of the backscattered signal.

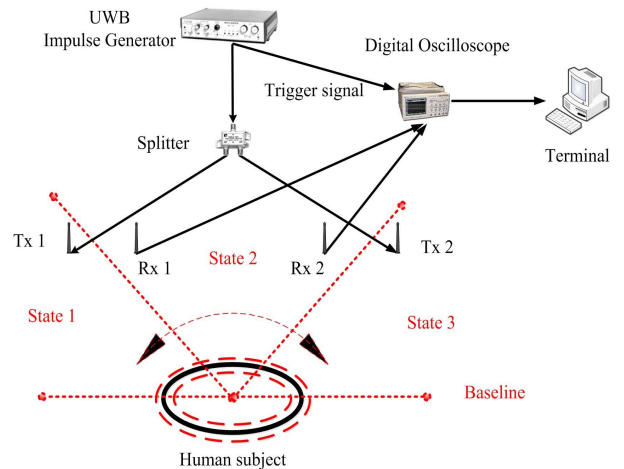


Fig. 1. System architecture.

Let a transmission frame be the time interval between two transmitted UWB pulses, and suppose that transmission frames are indexed by  $t = 0, \dots, T$ . For each frame, a peak detection technique is applied to the received UWB pulse waveform to estimate the propagation delay. We refer the reader to [19] for a detailed discussion of this detection procedure. Consider a transceiver pair  $j$ , where  $j = 1, 2$ , at transmission frame  $t$ . Let  $\tau_j(t)$  denote the propagation delay of the peak of the backscattered signal at the receiver. The subject may face different directions during the monitoring process. Because of the limited beam width of the receive antenna, backscattered signals from the subject's chest may not be detected by the antenna if she is facing certain directions. Let  $\rho(t)$  be a state variable that corresponds to the direction the subject is facing. Let  $D_j$  be the set of directions that result in backscattered signals that are within the beam width of receive antenna  $j$ . We consider the cases where  $\rho(t) \in D_j$  and  $\rho(t) \notin D_j$  separately.

Suppose that the backscattered signal is within the beam width of the receive antenna of transceiver pair  $j$ . Let  $d_{Tj}$  be the distance between the transmit antenna and reference chest wall position,<sup>1</sup> and  $d_{Rj}$  be the distance between the reference chest wall position and the receive antenna. The chest wall displacement about its reference position during transmission frame  $t$  is denoted as  $d(t)$ . The distance traveled by the UWB signal between the transmitter and receiver is then approximately  $d_{Tj} + d_{Rj} + 2d(t) + 2\nu_j(\rho(t))$ , where  $\nu_j(\rho(t))$  is an adjustment to the distance  $d_{Tj} + d_{Rj}$  as a result of the subject facing a particular direction  $\rho(t)$ . The term  $\nu_j(\rho(t))$  depends on where the antennas are placed with respect to the subject, and will be treated as an unknown nuisance parameter to be estimated from the measurements. The propagation delay

<sup>1</sup>As we are interested only in the variations in the chest wall movement, any reasonable reference position can be used without affecting our results. See Section II-B for more details.

of the UWB signal can be expressed as

$$\tau_j(t) = \frac{d_{Tj} + d_{Rj} + 2d(t) + 2\nu_j(\rho(t))}{c}, \quad (1)$$

where  $c$  is the speed of light in free space. The RSS of the UWB signal can be modeled as <sup>2</sup>

$$z_j(t) = -10\gamma \log \tau_j(t) + \beta, \quad (2)$$

where  $\gamma$  is the two way path loss exponent, and  $\beta = 10 \log P_t + K$  is a constant that depends on the power  $P_t$  of the transmit antenna and a propagation constant  $K$  that depends on the indoor path loss model that we adopt [22].

Suppose now that the backscattered signal is outside the beam width of the receive antenna. The backscattered signal detected by the receive antenna is due to ambient noise and backscattering from objects in the room where the experiment is conducted. It therefore has very low RSS and a large propagation delay. We model the propagation delay and RSS as constant unknown nuisance parameters.

### B. HMM for Chest Wall Motion Tracking

We develop a HMM to jointly estimate the direction that the subject is facing and the chest wall movements from the RSS-propagation delay profile of the backscattered signals. The subject's breathing can be modeled using different breathing modes. For example, one mode corresponds to the case where the subject stops breathing. Another mode corresponds to outward chest wall expansion during normal breathing, while a third mode corresponds to normal inward chest wall contraction. Additional modes like abnormal fast breathing and so on can be used to model the breathing pattern depending on the specific application under consideration. In Section III-A, we will group these modes into segments to detect changes in the breathing pattern. Let  $m(t)$  be the breathing mode at time frame  $t$ , and

$$\mathbf{S}(t) = [d(t), \rho(t)]^T. \quad (3)$$

We assume that breathing modes are independent. Furthermore, we suppose that  $\mathbf{S}(t)$  depends only on  $\mathbf{S}(t-1)$  and  $m(t)$ . (An example of such a model is where  $\rho(0), \dots, \rho(T)$  forms a Markov chain, independent of the chest wall displacements  $d(t)$ , and the distribution of  $d(t)$  depends only on the previous chest wall displacement  $d(t-1)$  and the current breathing mode  $m(t)$ .) Let  $\mathcal{F}_t = \{\mathbf{S}(u), u < t\}$ . Since  $m(t)$  is independent of  $\mathcal{F}_{t-1}$ , the conditional distribution of  $\mathbf{S}(t)$  is

$$\begin{aligned} p(\mathbf{S}(t) | \mathbf{S}(t-1), \mathcal{F}_{t-1}) \\ &= E[p(\mathbf{S}(t) | \mathbf{S}(t-1), \mathcal{F}_{t-1}, m(t)) | \mathbf{S}(t-1), \mathcal{F}_{t-1}] \\ &= E[p(\mathbf{S}(t) | \mathbf{S}(t-1), m(t)) | \mathbf{S}(t-1)] \\ &= p(\mathbf{S}(t) | \mathbf{S}(t-1)), \end{aligned}$$

so that  $\mathbf{S}(0), \mathbf{S}(1), \dots, \mathbf{S}(T)$  forms a Markov chain. We take  $\mathbf{S}(t)$  to be the hidden state of our HMM at time frame  $t$ . We discretize  $\rho(t)$  into three states to limit the complexity of the estimation procedure. Specifically, we let  $\rho(t) = 1$  if the subject is facing towards receiver 1,  $\rho(t) = 2$  if subject is

facing towards the midpoint between receivers 1 and 2, and  $\rho(t) = 3$  if she is facing towards receiver 2 (see Figure 1). We quantize the distance  $d(t)$  into  $M$  states. The transition matrix of the states of our HMM is then given by a  $3M \times 3M$  state transition matrix  $\mathbf{A}$ .

For each transceiver pair  $j = 1, 2$ , let  $\tau_{j,ref} = d_{Tj} + d_{Rj}$  be the propagation delay of a reference transmission frame, which is chosen to be a frame in which the receive antenna is able to detect a backscattered signal from the subject's chest wall.<sup>3</sup> Without loss of generality, we assume this to be the first transmission frame  $t = 0$ .<sup>4</sup> Let  $z_{j,ref}$  be the RSS of the signal in the reference transmission frame. The observed variables in transmission frame  $t = 1, \dots, T$ , are the relative delay and RSS. The relative delay is given by

$$\begin{aligned} \Delta_j(t) &= \frac{1}{2}(\tau_j(t) - \tau_{j,ref}) \\ &= \begin{cases} \frac{d(t) + \nu_j(\rho(t))}{c}, & \text{if } \rho(t) \in D_j, \\ \frac{\nu_j(\rho(t))}{c}, & \text{otherwise,} \end{cases} \end{aligned} \quad (4)$$

where  $\nu_j(\rho(t))/c$  is defined to be the relative propagation delay if  $\rho(t) \notin D_j$ . The relative RSS difference is given by

$$\begin{aligned} \Psi_j(t) &= z_j(t) - z_{j,ref} \\ &= \begin{cases} \psi_j(t), & \text{if } \rho(t) \in D_j, \\ \alpha_j, & \text{otherwise,} \end{cases} \end{aligned} \quad (5)$$

where  $\psi_j(t) = -10\gamma \log(1 + (2(d(t) + \nu_j(\rho(t))))/\tau_{j,ref})$ , and  $\alpha_j$  is a nuisance parameter to be estimated. The equations (4) and (5) are derived without any measurement noise. We now impose a stochastic model on the relative delay and relative RSS difference. For  $t = 1, \dots, T$ , let

$$\mathbf{O}(t) = [\Delta(t), \Psi(t)]^T, \quad (6)$$

be a sequence of vector observations with  $\Delta(t) = [\Delta_1(t), \Delta_2(t)] + n_\Delta(t)$ , and  $\Psi(t) = [\Psi_1(t), \Psi_2(t)] + n_\Psi(t)$ , where  $n_\Delta(t)$  and  $n_\Psi(t)$  are independent Gaussian random vectors when conditioned on  $\mathbf{S}(t)$ . Specifically, the conditional distribution of  $\Delta(t)$  is given by

$$p(\Delta(t) | \mathbf{S}(t)) \sim \mathcal{N}\left(\frac{\mu(t)}{c}, \Sigma\right) \quad (7)$$

with

$$\mu(t) = \begin{cases} [d(t), 0]^T + \mu_1, & \text{if } \rho(t) = 1, \\ [d(t), d(t)]^T + \mu_2, & \text{if } \rho(t) = 2, \\ [0, d(t)]^T + \mu_3, & \text{if } \rho(t) = 3, \end{cases} \quad (8)$$

where  $\mu_{\rho(t)} = [\nu_1(\rho(t)), \nu_2(\rho(t))]^T$ , and  $\Sigma$  is a covariance matrix. Similarly, the conditional distribution of  $\Psi(t)$  is given by

$$p(\Psi(t) | \mathbf{S}(t)) \sim \mathcal{N}(\psi(t), \Omega) \quad (9)$$

where

$$\psi(t) = \begin{cases} [\psi_1(t), \alpha_2]^T, & \text{if } \rho(t) = 1, \\ [\psi_1(t), \psi_2(t)]^T, & \text{if } \rho(t) = 2, \\ [\alpha_1, \psi_2(t)]^T, & \text{if } \rho(t) = 3, \end{cases} \quad (10)$$

<sup>3</sup>This can be done by performing a simple threshold test on the received signal peak.

<sup>4</sup>To ensure reference frames can be chosen for all antenna pairs, a calibration phase can be enforced.

<sup>2</sup>The symbol log denotes logarithm to the base 10.

and  $\Omega$  is a covariance matrix. Figure 2 shows our proposed HMM.

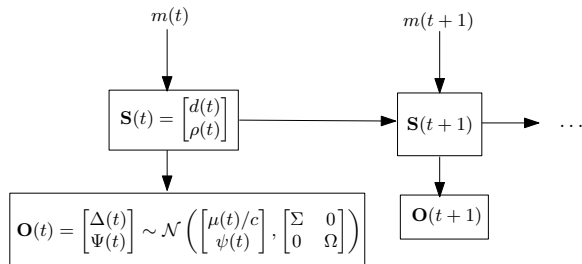


Fig. 2. HMM for chest wall motion tracking.

Given the observations  $\{\mathbf{O}(t) : t = 1, \dots, T\}$ , we apply the Baum-Welch algorithm [23] to obtain the transition probabilities of our state variable. We then use the Expectation-Maximization (EM) algorithm to estimate the parameters for our HMM. These two steps are repeated till the transition probabilities converge. Finally, the Viterbi algorithm [24] is used to obtain the most likely evolution of the state  $\mathbf{S}(t)$ . This procedure is summarized in the HRT algorithm.

---

#### HRT algorithm : HMM based Respiratory Tracking (HRT).

---

**Initialize:** state transition matrix  $\mathbf{A}$ ,  $\{\mu_k, k = 1, 2, 3\}$ ,  $\{\alpha_j, j = 1, 2\}$ ,  $\Sigma$  and  $\Omega$

**Data:**  $\{\mathbf{O}(1), \mathbf{O}(1), \dots, \mathbf{O}(T)\}$

**repeat**

    Obtain  $\mathbf{A}^{\text{new}}$  using Baum-Welch Algorithm

    Update  $\mathbf{A} \leftarrow \mathbf{A}^{\text{new}}$

    Estimate  $\{\mu_k, k = 1, 2, 3\}$ ,  $\{\alpha_j, j = 1, 2\}$ ,  $\Sigma$  and  $\Omega$  using EM algorithm.

**until**  $\mathbf{A}$  converges

Estimate sequence of states  $\{\mathbf{S}(1), \dots, \mathbf{S}(T)\}$  using Viterbi algorithm.

---

### III. BREATHING PATTERN SEGMENTATION

In this section, we present a signal segmentation algorithm to automatically segment the time series output of the HMM estimation procedure in Section II-B into periods of normal and disordered breathing, if any. We model the subject's breathing pattern with a linear regression model, with different parameters for normal and disordered breathing. Our goal is to estimate the positions (change points) in the output of the HRT algorithm at which there is a change in the regression model parameters. Our approach is based on the perfect simulation algorithm of [25].

#### A. Model Representation

Recall that we model the subject's breathing using different modes. These breathing modes can be grouped into categories or breathing patterns like normal and disordered breathing. Our objective in this section is to detect changes in the breathing pattern. Let  $y(t)$  be the estimate of the subject's chest wall displacement  $d(t)$  obtained using the HRT algorithm. Let  $\mathbf{y}(i : j) = (y(i), y(i+1), \dots, y(j))$  be a segment of the estimates

from transmission frames  $i$  to  $j$ . Suppose that  $\mathbf{y}(1 : T)$  can be divided into  $m$  segments, separated by the change points  $\delta_0, \delta_1, \dots, \delta_m$  with  $\delta_0 = 0$  and  $\delta_m = T$ . For each segment  $\mathbf{y}((\delta_i + 1) : \delta_{i+1})$ ,  $i = 0, \dots, m - 1$ , i.e., conditioned on the subject maintaining the same breathing pattern in this segment, we assume a linear regression model with order  $r_i$  given by

$$\mathbf{y}((\delta_i + 1) : \delta_{i+1}) = \mathbf{G}_i^{(r_i)} \beta_i + \epsilon((\delta_i + 1) : \delta_{i+1}), \quad (11)$$

where  $\mathbf{G}_i^{(r_i)}$  is a matrix of basis vectors,  $\beta_i$  is a vector of parameters, and  $\epsilon((\delta_i + 1) : \delta_{i+1})$  is a vector of independent and identically distributed random variables with mean 0 and the variance  $\varrho_i^2$ .

We now describe how the basis vectors in  $\mathbf{G}_i^{(r_i)}$  are chosen. The chest movement of a human while breathing can be approximated by sinusoids [26]. For each human subject, we perform a discrete time Fourier transform (DTFT) of her normal breathing pattern to obtain a set of dominant frequencies  $\{f_1, \dots, f_k\}$  by keeping only those frequencies whose DTFT coefficients are above a certain threshold. The threshold is chosen so that we typically have a set of 2 to 3 dominant frequencies in order to limit the complexity of our estimation. The basis matrix of order 1 is then defined to be

$$\mathbf{G}_i^{(1)} = [\mathbf{1} \ \mathbf{b}_i(f_1) \ \dots \ \mathbf{b}_i(f_k)],$$

where  $\mathbf{1}$  is a vector of all 1s, and

$$\mathbf{b}_i(f) = \begin{bmatrix} \sin(2\pi f(\delta_i + 1)) & \cos(2\pi f(\delta_i + 1)) \\ \sin(2\pi f(\delta_i + 2)) & \cos(2\pi f(\delta_i + 2)) \\ \vdots & \vdots \\ \sin(2\pi f\delta_{i+1}) & \cos(2\pi f\delta_{i+1}) \end{bmatrix}.$$

Disordered breathing is characterized by deviations in either amplitude or frequencies of the breathing pattern from that produced by normal breathing [19], and the subject may experience shallow or nonexistent breathing (apnea) or faster breathing (hyperpnea). The amplitude of the sinusoidal model is given by  $\beta_i$  in (11), which can be estimated for each segment. The frequencies are controlled by the basis matrix  $\mathbf{G}_i^{(r_i)}$ . To model hyperpnea (higher frequencies), we include higher order frequency terms in  $\mathbf{G}_i^{(r_i)}$  by letting

$$\mathbf{G}_i^{(p)} = [\mathbf{G}_i^{(p-1)} \ \mathbf{b}_i(pf_1) \ \dots \ \mathbf{b}_i(pf_k)],$$

for  $p > 1$ . The number and positions of the change points and the order, parameters, and variance of the regression model for each segment are all assumed to be unknown. Our goal is to obtain the maximum a posteriori (MAP) estimates of the parameters  $m$ , and  $\{\delta_i : i = 1, \dots, m - 1\}$ .

#### B. Perfect Simulation

The model in (11) has no analytical form for the posterior distributions of the parameters that we are interested in. We therefore use Monte Carlo methods to perform Bayesian inference [27], [28]. The most common approach is the use of Markov chain Monte Carlo (MCMC) techniques. However MCMC methods have the disadvantage of not being able to accurately determine if the procedure has converged, which may produce erroneous results [25]. In our setup, the observations

in disjoint segments are independent of each other, therefore we can adopt the so called perfect simulation approach of [25], [29], which involves drawing independent samples from the true posterior distribution, and hence avoiding issues of convergence. In the following, we describe briefly the perfect simulation algorithm, and refer the reader to [25] for details.

We impose an Inverse-Gamma prior distribution with shape parameter  $\varsigma/2$  and scale parameter  $\vartheta/2$  on  $\varrho_i^2$ , the variance of the noise variables in (11). For the  $j$ th component in the regression parameter vector  $\beta_i$ , we use an independent normal distribution  $\mathcal{N}(0, \varrho_i^2 \xi_j^2)$  as the prior, where  $\xi_j$  is a fixed parameter. Furthermore, we assume that the model orders  $r_i$  are bounded by a maximum order  $r$ , and we use a uniform prior for the model order of each segment. Since we have assumed that the breathing modes of every time frame are independent, the prior on the change points is a geometric distribution, with density function given by

$$f(m, \delta_1, \dots, \delta_{m-1}) = \lambda^{m-1} (1 - \lambda)^{n-m},$$

where  $\lambda$  is a fixed parameter. The parameters  $(\varsigma, \vartheta, (\xi_j)_{j=1}^{2r+1}, \lambda)$  can be chosen using a recursive procedure described in [25].

In the following, we present some formulas that allow us to compute the posterior probability of a change point. We refer the reader to [25] for the derivations. Let  $\Pr(t, s, q)$  be the conditional probability of the observations  $\mathbf{y}(t : s)$ , given that the model order is  $q$ . It can be shown that

$$\begin{aligned} \Pr(t, s, q) &= \mathbb{P}(\mathbf{y}(t : s) \mid t : s \text{ is a segment with order } q) \\ &= \Upsilon^{1/2} (\varsigma + \|\mathbf{y}\|_{\mathbf{Q}}^2)^{\frac{\vartheta+s-t+1}{2}} \\ &\quad \times \frac{\Gamma(\frac{\vartheta+s-t+1}{2})^{2q+1}}{\Gamma(\frac{\vartheta}{2})} \prod_{j=1}^{2q+1} \xi_j^{-1}, \end{aligned} \quad (12)$$

where  $\Upsilon = (\mathbf{G}^T \mathbf{G} + \mathbf{D}^{-1})^{-1}$ ,  $\mathbf{Q} = \mathbf{I} - \mathbf{G} \Upsilon \mathbf{G}^T$ ,  $\|\mathbf{y}\|_{\mathbf{Q}}^2 = \mathbf{y}^T \mathbf{Q} \mathbf{y}$ .

Let  $Q(t)$  be the conditional distribution of observing  $\mathbf{y}(t : T)$  given that there is a change point at  $t - 1$ . This can be calculated recursively using

$$\begin{aligned} Q(t) &= \frac{1}{r} \sum_{k=t}^{T-1} \sum_{q=1}^r \Pr(t, k, q) Q(t+1) \lambda (1 - \lambda)^{k-t} \\ &\quad + \frac{1}{r} \sum_{q=1}^r \Pr(t, T, q) (1 - \lambda)^{T-t}. \end{aligned} \quad (13)$$

The conditional probability of the next change point given that the previous one occurred at  $t - 1$  is then given by

$$\begin{aligned} &\mathbb{P}(\delta_j = s \mid \delta_{j-1} = t - 1, \mathbf{y}(1 : T)) \\ &\propto \frac{1}{r} \sum_{q=1}^r \Pr(t, s, q) Q(t+1) \lambda (1 - \lambda)^{s-t}. \end{aligned} \quad (14)$$

and

$$\begin{aligned} &\mathbb{P}(\delta_j = T \mid \delta_{j-1} = t - 1, \mathbf{y}(1 : T)) \\ &\propto \frac{1}{r} \sum_{q=1}^r \Pr(t, T, q) (1 - \lambda)^{T-t}. \end{aligned} \quad (15)$$

Making use of Equations (14) and (15), we can simulate the next change point given the previous one until the last data point. This constitutes one run of the simulation process. We repeat this process several times and accumulate the count of the number of times a particular point is determined to be a change point. We divide this count by the total number of runs and to obtain the posterior probability that this point is a change point. To find the MAP estimate of the change points, we use a Viterbi algorithm, with the additional constraint that no two change points are within a window of 2 seconds to reflect the fact that typical breathing segments are at least 2 seconds long. This procedure is formally presented in the BPS algorithm. We note that although this algorithm does not explicitly classify the segments into normal and disordered breathing segments, it allows us to estimate the number of apnea or hyponea episodes by taking into consideration other features like average amplitude and frequency in the segment.

---

#### BPS algorithm : Breathing Pattern Segmentation (BPS).

---

##### 1: Simulation

---

- 2: Calculate  $Q(t)$  for  $t = 1, \dots, T$  using (13).
  - 3: Initialize  $\delta_0 = 0$  and count vector  $c(1 : T) = (0, \dots, 0)$ .
  - 4: **for** Iter = 1,  $\dots$ ,  $N$  **do**
  - 5:    $i = 0$
  - 6:   **while**  $\delta_i < T$  **do**
  - 7:     Simulate  $\delta_{i+1}$  from (14) and (15).
  - 8:     Increment  $c(\delta_{i+1})$  by 1.
  - 9:      $i = i + 1$ .
  - 10:   **end while**
  - 11: **end for**
  - 12:  $c(1 : T) = c(1 : T)/N$ .
- 

##### 13: Viterbi Algorithm

---

- 14: Initialize  $Q^*(T + 1) = 1$ .
  - 15: **for**  $t = T, T - 1, \dots, 1$  **do**
  - 16:    $Q^*(t) = \frac{1}{r} \max_{\substack{t \leq s \leq T \\ 1 \leq q \leq r}} \Pr(t, s, q) Q^*(s+1) \lambda^{1(s \neq T)} (1 - \lambda)^{s-t}$
  - 17:   Set  $s^*(t)$  and  $q^*(t)$  to be the maximizers for  $Q^*(t)$ .
  - 18: **end for**
  - 19: Initialize  $\delta_0^* = 0$  and  $j = 0$ .
  - 20: **while**  $\delta_j^* < T$  **do**
  - 21:   Set  $\delta_{j+1}^* = s^*(\delta_j^* + 1)$  and  $q_{j+1}^* = q^*(\delta_j^* + 1)$ .
  - 22:    $j = j + 1$ .
  - 23: **end while**
  - 24: Number of change points  $m = j$ .
  - 25: For each  $\delta$  in  $(\delta_1^*, \dots, \delta_m^*)$ , if there are other change points within 1 second of  $\delta$ , keep only the change point with the highest  $c(\delta)$ . Update  $m$  accordingly.
- 

## IV. SIMULATION AND EXPERIMENTAL RESULTS

We verify the accuracy of the proposed HMM and the change point detection algorithm through both experimental and simulation studies. We implement the system model shown in Figure 1 with the experimental setup shown in Figure



Fig. 3. IR UWB experimental setup.

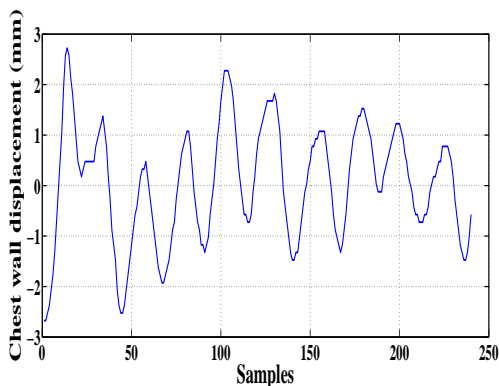


Fig. 4. Extracted chest wall displacement by RIP belt measurement.

3. The transmission frequency is approximately 4.2 GHz. In order to mitigate the effect of scattering from the surrounding clutter sources, we use a template subtraction method. In this method, we capture the received signal containing the human subject and subtract from it a reference or template signal which is recorded before the presence of the human subject. We perform peak detection on the received backscattered signal by fixing a threshold on the received signal strength. We quantize  $d(t)$ , the observed RSS and propagation delays levels into  $M = 10$ ,  $N = 4$  and  $K = 4$  levels respectively.

#### A. Simulation results

In this section, we perform simulations to verify the performance of our proposed algorithms. We assume a path loss exponent  $\gamma = 4.8$  and  $K = -25$  dB in (2) to take into account possible multipath effects. In each simulation run, we simulate 6 minutes long measurements, with a change in the facing direction of the subject every 2 minutes. Three types of breathing modes normal, fast and nonexistent breathing are randomly chosen throughout the 6-minute period, with each mode lasting for a random duration. In order to make the simulation more realistic we use 10 sets of chest displacements extracted from measurements by a RIP belt as the normal breathing pattern (see Figure 4 for an example). We use the Philips Respironics ALICE PDX diagnostic system for conducting the RIP belt measurements. For each of these patterns and for a fixed SNR, we generate 100 simulated

patterns by adding Gaussian noise to the pattern, and adjusting the amplitude and frequencies to simulate fast and nonexistent breathing modes. In addition, we simulate random changes in the facing direction of the subject using the path loss model in (2). The HMM algorithm is used to track the chest wall motion and the change point detection algorithm is used to detect the changes in the simulated breathing pattern as shown in Figure 6.

We calculate the root mean squared error (RMSE) between the actual chest wall displacement and the chest wall displacement estimated by the HRT algorithm. This RMSE is averaged over all the breathing patterns and all the corresponding chest wall displacements and is plotted against varying noise floors as shown in Figure 7. From Figure 7 at a moderate SNR value of 15 dB, we observe that the RMSE is approximately 0.7 mm, which suggests that the predicted chest wall motion by the HMM is fairly accurate.

We estimate the change point of the time series using the BPS algorithm. Figure 6 shows an example output with the predicted change points in the time series. The average time lag to detect a change point for each data set has also been plotted against varying noise floors as shown in Figure 8. It can be seen that the average time lag is approximately 0.4 seconds at 15 dB. Figure 9 shows the receiver operating characteristic (ROC) plot. In this simulation, we simulated 180 instances of the chest wall motion with randomly placed apnea episodes. The change point algorithm was then tested to identify the time instant of change in the respiratory effort. This process was repeated for varying levels of SNR. For a particular SNR, the probability of detection is calculated by counting the number of times the algorithm accurately predicted a change point to within 1 sec. A change point appearing outside the window was considered to be a missed detection. Similarly the probability of false alarm was calculated by counting the number of times a false positive was registered within the time window. As seen from Figure 9, at a typical SNR value of 15 dB the BPS algorithm detects a change point about 85% of the time correctly, with false alarms happening about 5% of the time.

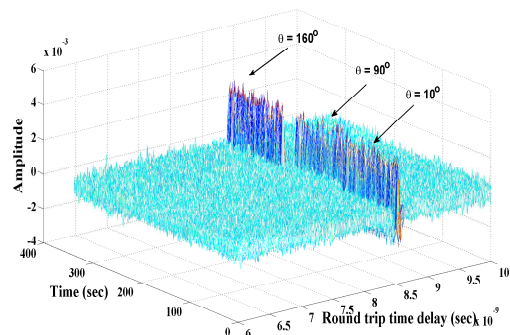


Fig. 5. Simulated RSS-delay profile of a subject changing facing direction.

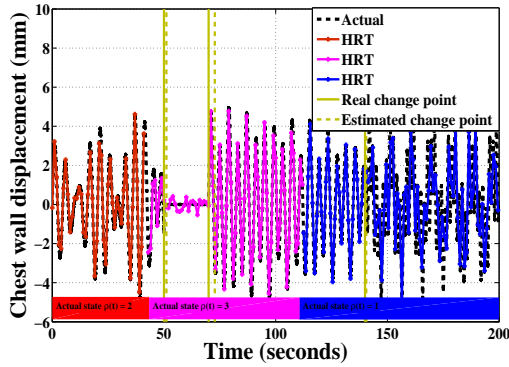


Fig. 6. Predicted chest wall motion and underlying states by the proposed HMM. Different colors for the HRT curve correspond to different state estimates for the subject facing direction  $\rho(t)$ .

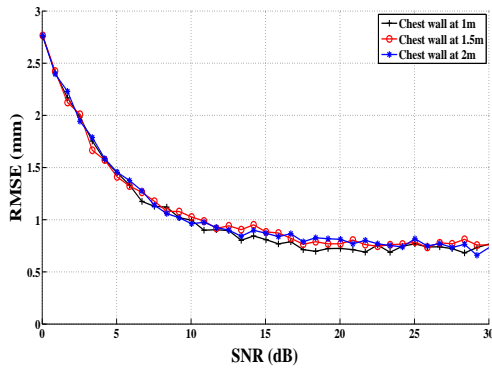


Fig. 7. RMSE result for 100 iterations at varying noise floors.

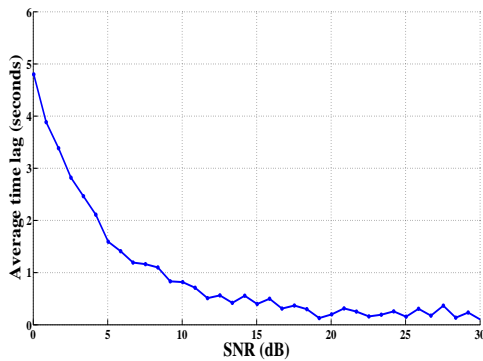


Fig. 8. Average time lag for change point detection on simulated data sets for varying noise floors.

### B. Comparison with RIP Belt

In order to evaluate our proposed algorithms empirically, we recruit 15 human volunteers to test our UWB respiratory monitoring system. We compare the performance of our UWB respiratory system with the medical gold standard using a RIP belt measurement system. Each volunteer is asked to breathe normally for a duration of 30 seconds, and then hold her breath for a duration of 10 seconds. At the end of these 40 seconds, the volunteer changes her facing direction randomly, and repeats the process. While performing these measurements, we

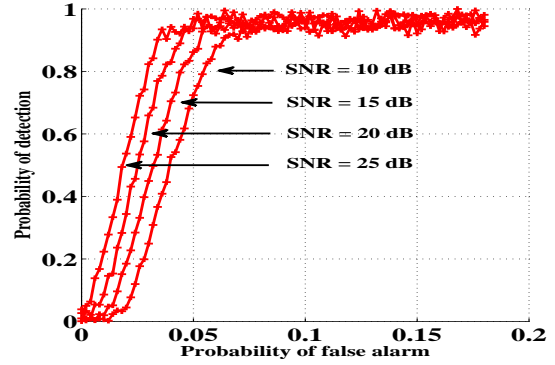


Fig. 9. ROC curve for the change point detection algorithm.

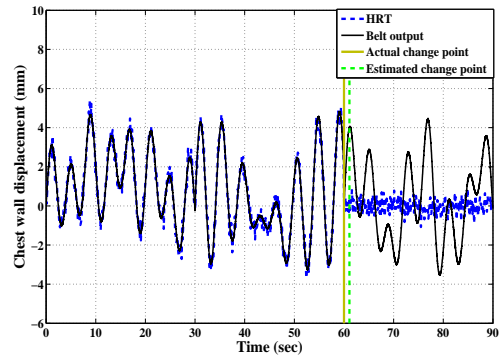


Fig. 10. Estimated chest wall motion based upon signal at receiver 1 alone. Human subject changes facing direction every 30 seconds.

simultaneously measure the chest wall motion of the volunteer using the RIP belt.

The antennas dimensions are 3 cm width, and 4 cm height. The gain is 11 dB with azimuth beamwidth of  $60^\circ$  and an elevation beamwidth of  $40^\circ$ . The UWB pulses are generated using the Picosecond Pulse Labs' 3500D impulse generator, which produces Gaussian pulses with a pulse width of 80 ps. An Agilent DSO81204B real-time wideband digital oscilloscope with a sampling rate of 40 GHz is used for recording the back-scattered signal from the human chest. The bandwidth

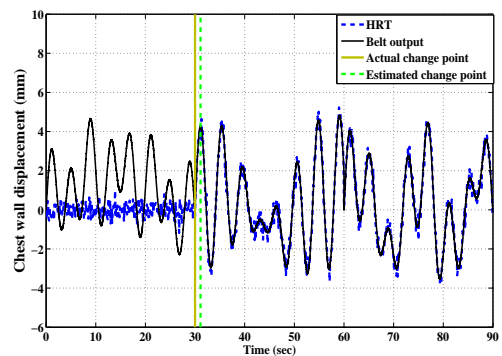


Fig. 11. Estimated chest wall motion based upon signal at receiver 2 alone. Human subject changes facing direction every 30 seconds.



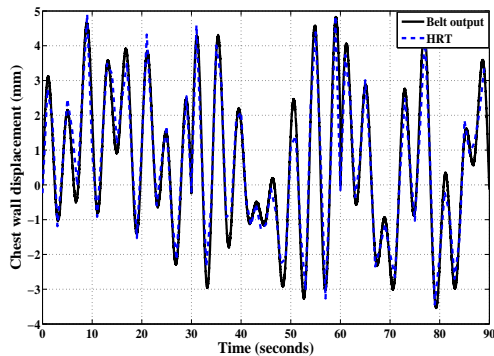


Fig. 12. Estimated chest wall motion when the human subject changes facing direction based on received signal at both the receivers.

of the signal is approximately 4 GHz. The antenna return loss measured with an Agilent N5230A vector analyzer is higher than 10 dB. The transmission power in the experiments is well below the FCC regulation for UWB medical applications. The distance between transceiver units is approximately 10 cm, and the distance between the subject and transceiver units is varied from 1 to 3 m.

Table I shows the cross-correlation between our estimated chest wall motion with the RIP belt measurements. The average degree of correlation between these two estimated chest wall displacements is 81.4%, which indicates that the HMM algorithm is fairly accurate and comparable in its performance with the RIP belt.

Figures 10 and 11 show the estimated chest wall motion and detected change points using the HRT algorithm and BPS algorithm algorithms respectively. The human subject is asked to change her facing direction after every 30 seconds with normal breathing during the entire duration. The change points in Figure 10 and 11 are due to the change in the facing direction of the human subject and do not correspond to cessations or variations in the subject's breathing. No change points are detected in Figure 12, which is produced using the HRT algorithm on data from both receivers. This shows the advantage of the proposed multiple transceiver set-up and the HRT algorithm in avoiding any false alarms in change point detection due to the change in facing direction of the human subject.

We ask the volunteers to move laterally along the baseline over distances of 20, 40, and 50 cm to simulate lateral shifts in subjects' position during respiratory monitoring. Table II shows a graceful degradation of cross-correlation between the HRT output and the RIP belt output as the lateral range increases. Figure 13 shows the simulated RMSE for various lateral ranges. We see that our method should only be used if the lateral motion is limited, e.g. when the patient is lying on a single bed, in which case lateral motions are expected to be less than 20 cm.

## V. CONCLUSION

We have designed a contactless and non-invasive UWB respiratory monitoring system using multiple transceivers in

TABLE I  
RESULTS FOR CHANGE POINT DETECTION ALGORITHM FOR 15 HUMAN SUBJECTS

Human subjects	RMSE (mm)	Change point detection delay (sec)	Cross-correlation coefficient
1	0.59	0.54	0.76
2	0.9	0.82	0.74
3	1.3	0.76	0.84
4	0.95	0.63	0.82
5	0.65	0.34	0.81
6	0.97	0.47	0.75
7	0.6	0.52	0.79
8	0.57	0.26	0.88
9	0.96	0.67	0.79
10	0.66	0.37	0.85
11	0.83	0.45	0.89
12	1.05	0.78	0.83
13	0.85	0.32	0.77
14	0.98	0.46	0.86
15	0.51	0.98	0.83
Average	0.825	0.558	0.814

TABLE II  
RESULTS FOR LATERAL MOTION EFFECT.

Lateral motion along baseline (cm)	Cross-correlation coefficient
20	0.73
40	0.71
50	0.65

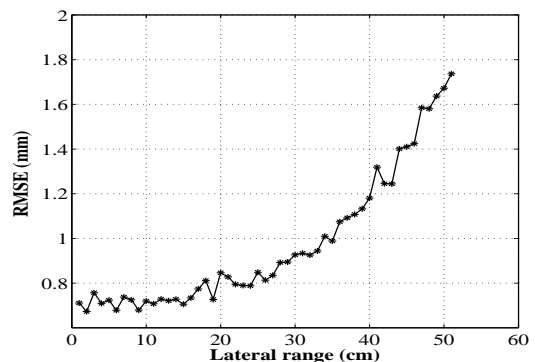


Fig. 13. Simulated RMSE at various lateral ranges, with SNR = 15 dB.

order to allow accurate respiratory monitoring regardless of the direction a subject is facing. We have developed algorithms to estimate and track a subject's respiratory motions from the backscattered signals at the UWB receivers, and an algorithm to segment the breathing patterns so that the number of apnea or hypnea episodes can be estimated. Our simulations and empirical experiments show that our system produces measurements highly correlated with the medical gold standard using RIP belts.

## REFERENCES

- [1] F. Nieto, T. Young, L. Lind, E. Shahar, J. Samet, S. Redline, R. D'Agostino, A. Newman, M. Lebowitz, and T. Pickering, "Association of sleep disordered breathing, sleep apnea, and hypertension in a large community-based study," *J. Amer. Med. Assoc.*, vol. 283, p. 18291836, 2000.
- [2] C. Guilleminault, S. Connolly, and R. Winkle, "Cardiac arrhythmia and conduction disturbances during sleep in 400 patients with sleep apnea syndrome 8," *Amer. J. Cardiol.*, vol. 52, no. 5, p. 490494, 1983.

- [3] W. Flemons, J. Remmers, and A. Gillis, "Sleep apnea and cardiac arrhythmias. is there a relationship?" *Amer. Rev. Respir. Dis.*, vol. 148, no. 3, p. 618621, 1993.
- [4] P. Philip, P. Sagaspe, E. Lagarde, D. Leger, M. Ohayon, B. Bioulac, J. Boussuge, and J. Taillard, "Sleep disorders and accidental risk in a large group of regular registered highway drivers," *J. Sleep Med.*, vol. 31, no. 3, pp. 1071–1078, 2010.
- [5] T. Young, L. Finn, P. Peppard, M. Szklo-Coxe, D. Austin, F. Nieto, R. Stubbs, and K. Hla, "Sleep disordered breathing and mortality: eighteen-year follow-up of the Wisconsin sleep cohort," *Sleep.*, vol. 31, no. 8, pp. 1071–1078, 2008.
- [6] N. Marshall, K. Wong, P. Liu, S. Cullen, M. Knuiman, and R. Grunstein, "Sleep apnea as an independent risk factor for all-cause mortality," *The busselton health study, sleep.*, vol. 31, no. 8, pp. 1079–1085, 2008.
- [7] C. Iber, S. Ancoli-Israel, and A. Chesson, "The AASM manual for the scoring of sleep and associated events," *American Academy of Sleep Medicine*, 2007.
- [8] T. Hoffmann, B. Eilebrecht, and S. Leonhardt, "Respiratory monitoring system on the basis of capacitive textile force sensors," *IEEE Sensors Journal*, vol. 11, no. 5, pp. 1112–1119, May 2011.
- [9] C. Merritt, H. Nagle, and E. Grant, "Textile-based capacitive sensors for respiration monitoring," *IEEE Sensors Journal*, vol. 9, no. 1, pp. 71–78, Jan. 2009.
- [10] A. Bianchi, M. Mendez, and S. Cerutti, "Processing of signals recorded through smart devices: sleep-quality assessment," *IEEE Transactions on Information Technology in Biomedicine*, vol. 14, no. 3, pp. 741–747, May 2010.
- [11] D. Townsend, R. Goubran, F. Knoefel, and J. Leech, "Validation of unobtrusive pressure sensor array for central sleep apnea screening," *IEEE Transactions on Instrumentation and Measurement*, vol. 61, no. 7, pp. 1857–1865, July 2012.
- [12] E. Staderini, "UWB radars in medicine," *IEEE Aerospace and Electronic Systems Magazine*, vol. 17, no. 1, pp. 13–18, Jan 2002.
- [13] D. Morgan and M. Zierdt, "Novel signal processing techniques for Doppler radar cardiopulmonary sensing," *Signal Processing*, vol. 89, no. 1, p. 4566, 2009.
- [14] I. Immoreev and T.-H. Tao, "UWB radar for patient monitoring," *IEEE Aerospace and Electronic Systems Magazine*, vol. 23, no. 11, pp. 11–18, Nov. 2008.
- [15] B. Gupta, E. Cianca, M. Ruggieri, and R. Prasad, "A novel FM-UWB system for vital sign monitoring and its comparison with IR-UWB," in *Proc. 2<sup>nd</sup> International Symposium on Applied Sciences in Biomedical and Communication Technologies, ISABEL 2009.*, Nov. 2009, pp. 1–4.
- [16] M. Otsu, R. Nakamura, and A. Kajiwara, "Remote respiration monitoring sensor using Stepped-FM," in *Proc. IEEE Sensors Applications Symposium (SAS)*, Feb. 2011, pp. 155–158.
- [17] K. Higashikaturagi, Y. Nakahata, I. Matsunami, and A. Kajiwara, "Non-invasive respiration monitoring sensor using UWB-IR," in *Proc. IEEE International Conference on Ultra-Wideband, ICUWB.*, vol. 1, Sept. 2008, pp. 101–104.
- [18] A. Lazaro, D. Girbau, R. Villarino, and A. Ramos, "Vital signs monitoring using impulse based UWB signal," in *Proc. 41<sup>st</sup> European Microwave Conference (EuMC)*, Oct. 2011, pp. 135–138.
- [19] J. Lai, Y. Xu, E. Gunawan, E. Chua, A. Maskooki, Y. L. Guan, K.-S. Low, C. B. Soh, and C.-L. Poh, "Wireless sensing of human respiratory parameters by low power Ultrawideband Impulse Radio Radar," *IEEE Transactions on Instrumentation and Measurement.*, vol. 60, no. 3, pp. 928–938, March 2011.
- [20] S. Gezici, "Theoretical limits for estimation of periodic movements in pulse-based UWB systems," *IEEE Journal of Selected Topics in Signal Processing.*, vol. 1, no. 3, pp. 405–417, Oct. 2007.
- [21] S. Gezici and O. Ankan, "Theoretical limits and a practical estimator for joint estimation of respiration and heartbeat rates using UWB Impulse Radio," in *Proc. IEEE International Conference on Ultra-Wideband, ICUWB.*, Sept. 2007, pp. 606–611.
- [22] S. Mazuelas, F. Lago, D. Gonzalez, A. Bahillo, J. Blas, P. Fernandez, R. Lorenzo, and E. Abril, "Dynamic estimation of optimum path-loss model in a RSS Positioning System," in *IEEE/ION Position, Location and Navigation Symposium*, May 2008, pp. 679–684.
- [23] L. Rabiner, "A tutorial on hidden Markov models and selected applications in speech recognition," *Proceedings of the IEEE*, vol. 77, no. 2, pp. 257–286, Feb 1989.
- [24] J. Forney, G.D., "The Viterbi algorithm," *Proceedings of the IEEE*, vol. 61, no. 3, pp. 268–278, March 1973.
- [25] P. Fearnhead, "Exact Bayesian curve fitting and signal segmentation," *IEEE Transactions on Signal Processing*, vol. 53, no. 6, pp. 2160–2166, June 2005.
- [26] Y. Chen, E. Gunawan, K. S. Low, C. Boon, C. B. Soh, and L. L. Thi, "Human respiration rate estimation using Body-worn UWB radar," in *IEEE Antennas and Propagation Society International Symposium, 2007*, June 2007, pp. 265–268.
- [27] T. Y. Yang and L. Kuo, "Bayesian binary segmentation procedure for a Poisson process with multiple changepoints," *Journal of Computational and Graphical Statistics*, vol. 10, pp. 772–785, 2001.
- [28] D. Barry and J. Hartigan, "A Bayesian analysis of change point problems," *Applied Statistics*, vol. 88, pp. 309–319, 1993.
- [29] P. Fearnhead, "Exact and efficient Bayesian inference for multiple changepoint problems," *Statistics and Computing*, vol. 16, pp. 203–213, 2006.